2025 IEEE Biomedical Circuits and Systems Conference (BioCAS) | 979-8-3315-7336-2/25/$31.00 ©2025 IEEE | DOI: 10.1109/BioCAS67066.2025.00099

Prediction of Acute Kidney Injury Onset using Electrocardiograph and Demographic data through Reservoir Computer On-Chip

Jose Sanchez*, Tushar Gupta*, Vasundhara Damodaran*, Imon Banerjee†, and Arindam Sanyal*
*School of Electrical, Computer and Energy Engineering, Arizona State University, AZ, USA.
†Mayo Clinic, Phoenix, AZ, USA.
Email: jcsanc12@asu.edu, tgupta39@asu.edu, vdamoda2@asu.edu, banerjee.imon@mayo.edu, arindam.sanyal@asu.edu

***Abstract*—Acute kidney injury (AKI) is a prevalent clinical concern, often leading to adverse outcomes such as elevated mortality and hospital readmission rates among patients. Disconcertingly, a significant care gap exists, with fewer than 10% of AKI patients obtaining nephrologist-led follow-up post-discharge care from the hospital. This work introduces an artificial intelligence (AI)-based methodology that synergistically combines single-lead electrocardiogram (ECG) data, demographic attributes, and creatinine levels to address this healthcare gap by forecasting AKI recurrence within a three-to-seven-day period prior to clinical diagnosis. The ECG signal is processed using a reservoir computer (RC) implemented on a 28nm CMOS test-chip, providing a compact representation that enhances predictive ability. Integrating demographic factors further refines the prediction, culminating in an accuracy of 81.2% when validated against retrospective patient data sourced from Mayo Clinic, across various locations.**

***Index Terms*—Machine learning, acute kidney injury, electrocardiogram, mixed-signal classifier, and reservoir-computer**

I. Introduction

Acute kidney injury (AKI) is frequently encountered in clinical settings and is associated with diminished long-term health outcomes, including increased risk of death and hospital readmission. A study revealed that 18% of AKI survivors were re-hospitalized, and 8% died within 30 days of discharge, with recurrent AKI being the leading cause [1]. Despite these worrying statistics, many patients opt out of specialized nephrological care, citing factors such as hospital fatigue and logistical challenges i.e. long travel times. To address this deficit in post-AKI management, this work proposes a home-based monitoring framework that employs artificial intelligence (AI) to predict AKI recurrence within a window of three to seven days prior to its clinical onset. The proposed system integrates electrocardiogram (ECG) readings with electronic medical record (EMR) data, including age, race, gender, weight, as well as initial creatinine levels recorded at the same time as the other EMR information. Fig. 1 gives an overview of this system. The core of the system features a reservoir computer (RC) that encodes single-lead ECG data into a condensed and information-rich format. The RC-based representation of the ECG signal, which is sensitive to electrolyte disturbances indicative of AKI [2], is concatenated with the creatinine and demographic data, to be processed by a neural network to estimate the likelihood of recurrence. The RC is fabricated using a 28nm CMOS process, while the fusion model is on software with the goal of future smartphone-based deployment. Encoding the ECG data at the sensor level minimizes radio frequency (RF) transmission, conserving battery life of the ECG sensor. This is feasible due to the RC's capability to derive salient features from sparse signals using a small number of neurons [3]. The rest of this paper is organized as following: Section II defines the dataset provided by Mayo Clinic that is used in this work, Section III discusses the proposed architecture and artificial intelligence model used, Section IV presents measurement results of the test-chip, and Section V concludes the discussion of this work.

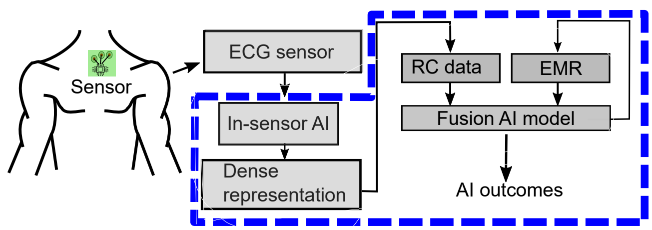

Fig. 1: Overview of the proposed technique for predicting AKI onset through ECG and demographic information inputs to an ANN; the work of this paper is enclosed within blue.

II. Dataset

The dataset comprises over 7100 retrospective patient records, from 1883 unique individuals, obtained from Mayo Clinic. Each ECG sample was recorded within three to seven days prior to either AKI diagnosis or normal status confirmation. The dataset includes 1118 male, and 765 female patients, with their ages ranging from 18 to 90 years. Fig. 2 details the demographic breakdown of the patient samples in this dataset (body mass index is given to indicate the distribution of the weights of the patient records). The dataset was divided into training and testing sets, ensuring that data from each patient appeared in only one set to maintain patient exclusivity. The training set included 1506 unique patients with 5670 ECG samples, and the test split contained 377 unique patients with 1495 ECG samples. For each patient, 12-lead ECGs, demographic, and creatinine level data were collected; however, only ECG data from V4 lead was used for model input as it gave the best model performance in software (see Table I). The ECG data was pre-processed by using a median filter, which suppresses noise of the ECG signal and reduces its size [4]. This step reduced noise while keeping the data volume low enough for direct input into the RC, eliminating the need for intermediate feature extraction, simplifying the circuit design by avoiding an on-chip feature extractor. Static demographic features - age, weight, race, and gender - were all scaled to the 0 to 1 range by normalizing age and weight, and one-hot-encoding race and gender. Fig. 2 shows the distribution of these features among the patient records. Also considered with the other EMR data was a baseline creatinine value for each patient sample. The RC output was concatenated with this data to be passed to the neural network off-chip.

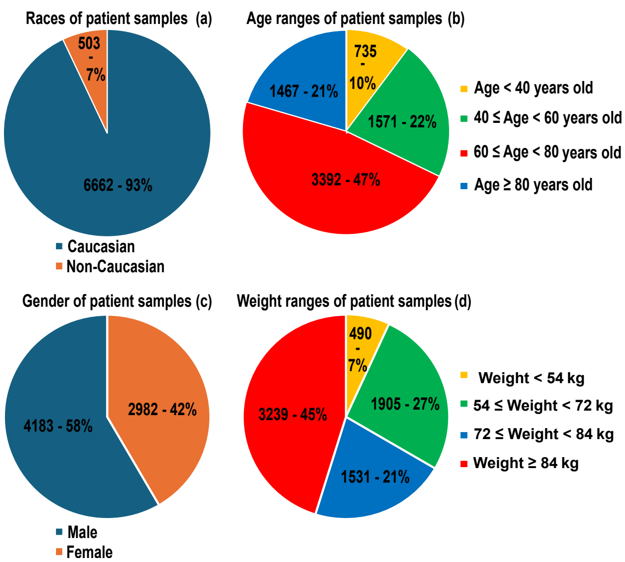

Fig. 2: Pie charts of patient samples according to a) race, b) age, c) gender, and d) weight.

TABLE I: Performance of different ECG lead data in software test accuracy.

Lead	I	II	III	V1	V2	V3	V4	V5	V6	AvF	AvR	AvL
Accuracy	0.822	0.820	0.825	0.816	0.817	0.822	**0.833**	0.825	0.823	0.822	0.825	0.819

III. Proposed Architecture

A. Overview of RC circuits

RC is a computational technique that projects input signals into a high-dimensional space through static nonlinear projections, which enhances class separation. A key advantage of RC is that it does not require training of the reservoir or input layers. Additionally, the inherent nonlinearity of RC eliminates the need for highly linear analog circuitry, thereby reducing energy consumption. RC compresses the sensor input and encodes it, reducing RF packet size and power. Prior RC implementations often relied on photonic or energy-intensive analog designs [5]–[8]. These works [5]–[7] require large capacitors, leading to energy inefficiency or needed background calibration for delay or nonlinearity elements. In a prior work [8] time-multiplexing was used on an on-chip analog RC to create multiple virtual neurons from a single physical neuron, thus avoiding requiring large capacitors or calibration. However, [8] used continuous-time circuits, which are are not energy efficient due to the slowly varying signals found in biomedical applications as they require large capacitors and have static energy consumption [9]. Hence, the key aspect of this work is the adoption of a low-power switched-capacitor-based RC system that builds on previous efforts by integrating all neurons on-chip and reducing energy consumption. For this work's RC parameters, simulations of the RC model were used to determine the optimal values for best performance as illustrated in Fig. 3.

B. Circuit design

The RC output with N neurons is defined as

$$\vec{R_k}[n] = H\left(G_i\vec{W_i} \times \vec{X}^T + G_f\vec{W_r} \times \vec{R_k}[n-1]\right) \quad (1)$$

here $\vec{X} = [X_1X_2\cdots X_D]$ represents the ECG signal with D samples, $\vec{W_i}$ is a $N \times D$ input weight matrix ($D >> N$), $\vec{W_r}$ is an $N \times N$ interconnection weight matrix for the reservoir layer, $H(\cdot)$ denotes the nonlinear activation, G_i and G_f are the input scaling and feedback gain factors respectively. The RC is constructed using a switched-capacitor integrator design, shown in Fig. 4. Each neuron functions as a leaky integrator, seen in (1), implemented with a low-gain amplifier ($\approx 25dB$). The neuron's output is reset whenever it crosses a predefined threshold. The architecture features lateral inhibition among clusters of three neurons, modeled after biological vision systems and aids in detecting transient signals such as the QRS complex in a ECG signal. Lateral inhibition is possible due to all the neurons in the same cluster being reset simultaneously. Sampling capacitors, C_{in}, C_{f1}, C_{f2}, are each 14.fF, while the feedback capacitor C_{intg} is 44.4fF. The ratio of the sampling capacitors to the feedback capacitor sets the feedback gain G_f. The input scaling factor G_i is realized off-chip along with the input layer. Input ECG data of 2500 time samples are compressed using 70 neurons, achieving a compression factor around 36. The nonlinear activation $H(\cdot)$ stems from the amplifier behavior in slew mode, reset dynamics in the integrator, and charge injection error from the switches, all of which are harnessed as part of the system's computational kernel. Hence, these proposed analog RC neurons can be extremely small in contrast to traditional analog design requirements of careful matching, large area, and high power to prevent mismatches and nonlinearity. Input multiplication occurs off-chip to allow for flexible testing with arbitrary input sample sizes D, with the input weight matrix $\vec{W_i}$ restricted to binary '1/0' values.

The analog outputs are serialized and digitized via a 10-bit successive approximation register analog-to-digital converter (SAR ADC), which uses bi-directional switching technique to minimize energy consumption [10]. ADC nonlinearities are absorbed by the RC's activation function, simplifying the ADC's design constraints.

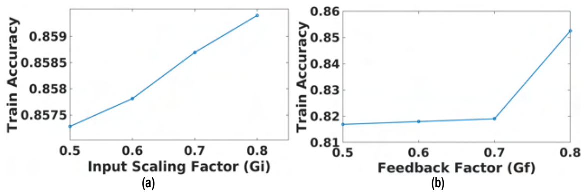

Fig. 3: Plots of train accuracy versus a) input scaling factor and b) feedback factor.

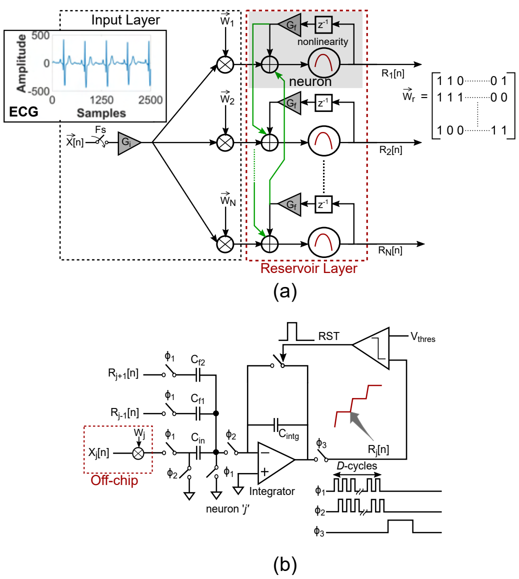

Fig. 4: Schematic of a) RC architecture; and b) single reservoir neuron.

C. ANN

The output of the RC neurons are sent to a neural network off-chip for predicting AKI onset. As previously discussed in Section II, demographic information - age, race, gender, weight, were used as well as a baseline creatinine measurement. All input data for the respective AI models were scaled to the range 0 to 1 by one-hot-encoding race and gender, and normalizing weight, age, and RC output. This ensures equal weighing of the input data when feed to the neural networks. The various neural networks tested were: logistic regression (LR), k-nearest-neighbor (KNN), support vector machine (SVM), and artificial neural network (ANN). The hyper-parameters of the neural networks were optimized by a grid search on the training dataset.

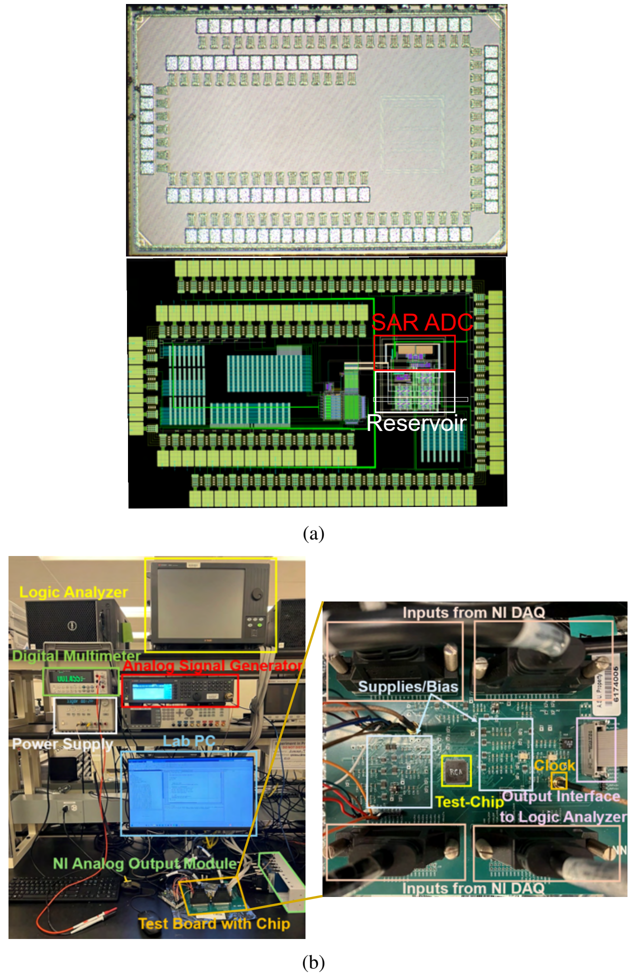

Fig. 5: a) Die photograph and layout view of the test-chip; b) picture of the test board with the chip and equipment interfaces.

IV. Measurement Results

The 28nm CMOS test-chip, including its layout is shown in Fig. 5. This test-chip was fabricated with dummy metal fills to meet process requirements. The resulting additional parasitics have negligible impact, as they are incorporated into the RC's nonlinearity. Power consumption was measured at 16.8μW at 0.9V with the RC operating at 31.25kHz and the SAR ADC at 2MHz. The core area is 1.65mm$\times$1.04mm. Fig. 5 shows the test board housing the test-chip, with the low-dropout regulators and potentiometers used to properly bias the test-chip, along with the equipment needed to capture the test-chip's outputs. Input signals were supplied via NI DAQ systems, and the outputs were recorded using a logic analyzer. The performance of the various models was assessed using confusion matrices. Their test accuracies are summarized in Table II, while the corresponding confusion matrices are presented in Fig. 6. Among the models, the ANN with a

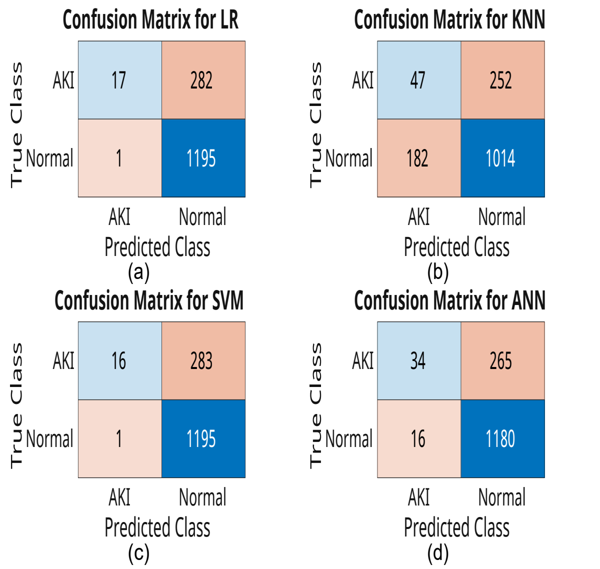

Fig. 6: Confusion Matrices of Test Results with various AI methods: a) Logistic Regression b) K-nearest neighbors c) Support Vector Machine and d) Artificial Neural Network.

single hidden layer comprising 298 neurons and a hyperbolic tangent activation function achieved the highest test accuracy. This ANN model also attained a precision of 0.817, sensitivity of 0.987, and a balanced F1 score of 0.894. Table III compares this work with state-of-the-art chronic kidney diseases (CKD)/AKI detection/onset prediction tools using ECG, EMR, and clinical data such as measurement results of biomedical markers such as fatty-acid binding protein, hemojuvelin, neutrophil gelatinase-associated lipocalin, etc. [11]. This work achieves results that are comparable to, or even better than, those of other works that utilize more extensive EMR and clinical data, despite relying solely on single-lead ECG data and minimal EMR information. The proposed analog RC achieves an energy consumption of 58nJ/inference including the input layer and RC layer, which as shown in Fig. 7 is competitive and on the lower end of energy/inference for other state-of-the-art technologies [12]–[30]. For the RC layer alone, this work achieves an energy consumption of just 0.5nJ/inference - the lowest value compared to the other works in Fig. 7. Compared to our previous work [30], which reported a similarly low energy/inference for the RC layer (1.5nJ/inference compared to 0.5nJ/inference), the earlier work resulted in lower model performance (test accuracy of 0.758 versus 0.812) and was evaluated on a much smaller dataset (295 samples from 117 unique patients, compared to 7165 samples from 1883 unique patients in this work). Overall, this work demonstrates both improved energy efficiency and superior classification performance.

V. Conclusion

This work has presented prediction of AKI recurrence three to seven days before onset, by utilizing single-lead ECG and demographic data as input data to an ANN. The proposed framework was validated using data given by Mayo Clinic. Its performance shows the potential of at-home monitoring for AKI patients using intelligent wearables.

TABLE II: Performance of different neural networks.

Model	Precision	Sensitivity	Accuracy	F1 Score
Logistic Regression	0.809	0.999	0.811	0.894
K-Nearest Neighbor	0.801	0.848	0.710	0.824
Support Vector Machine	0.809	0.999	0.810	0.894
Artificial Neural Network	0.817	0.987	0.812	0.894

TABLE III: Comparison with kidney disease detection tasks.

	Task	Predictor	Accuracy	Sensitivity
[11]	CSA-AKI onset	EMR and Clinical Data	0.822	0.813
[31]	AKI onset within 2 days	EMR	0.558	–
[32]	AKI in Heart Failure Patients	EMR and Clinical Data	0.884	0.960
This work	AKI onset within 3–7 days	1-lead ECG+EMR	0.812	0.987

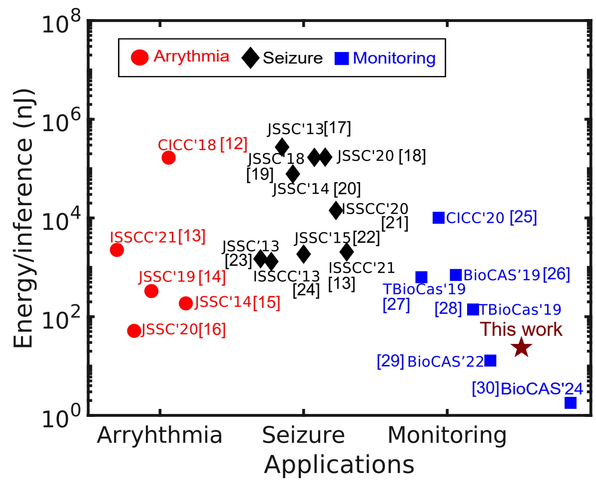

Fig. 7: Comparison with state-of-the-art AI ASICs for different bio-medical applications.

Acknowledgment

This work is supported by National Institutes of Health under grant number R01 EB035403-02, SRC through task number 3160.033, and Alphacore Inc. under DoE grant number DE-SC0022923.

References

[1] J. Vanmassenhove, R. Vanholder, and N. Lameire, "Points of concern in post acute kidney injury management," *Nephron*, vol. 138, no. 2, pp. 92–103, 2018.
[2] N. El-Sherif and G. Turitto, "Electrolyte disorders and arrhythmogenesis," *Cardiology Journal*, vol. 18, no. 3, pp. 233–245, 2011.
[3] M. Le Berre, E. Ressayre, A. Tallet, H. Gibbs, D. Kaplan, and M. Rose, "Conjecture on the dimensions of chaotic attractors of delayed-feedback dynamical systems," *Physical Review A*, vol. 35, no. 9, p. 4020, 1987.
[4] W. Hao, Y. Chen, and Y. Xin, "Ecg baseline wander correction by mean-median filter and discrete wavelet transform," in *Annual International Conference of the IEEE Engineering in Medicine and Biology Society (EMBC)*, 2011, pp. 2712–2715.
[5] F. C. Bauer, D. R. Muir, and G. Indiveri, "Real-time ultra-low power ECG anomaly detection using an event-driven neuromorphic processor," *IEEE Transactions on Biomedical Circuits and Systems*, vol. 13, no. 6, pp. 1575–1582, 2019.

[6] K. Bai and Y. Yi, "DFR: An energy-efficient analog delay feedback reservoir computing system for brain-inspired computing," *ACM Journal on Emerging Technologies in Computing Systems (JETC)*, vol. 14, no. 4, pp. 1–22, 2018.

[7] Y. Chen, E. Yao, and A. Basu, "A 128-channel extreme learning machine-based neural decoder for brain machine interfaces," *IEEE transactions on biomedical circuits and systems*, vol. 10, no. 3, pp. 679–692, 2015.

[8] S. T. Chandrasekaran, I. Banerjee, and A. Sanyal, "7.5 nJ/inference CMOS Echo State Network for Coronary Heart Disease prediction," in *IEEE European Solid-State Device Research Conference (ESSDERC)*, 2021, pp. 103–106.

[9] Y. Li, C. C. Y. Poon, and Y.-T. Zhang, "Analog integrated circuits design for processing physiological signals," *IEEE Reviews in Biomedical Engineering*, vol. 3, pp. 93–105, 2010.

[10] L. Chen, A. Sanyal, J. Ma, and N. Sun, "A 24-μW 11-bit 1-MS/s SAR ADC with a bidirectional single-side switching technique," in *IEEE European Solid State Circuits Conference (ESSCIRC)*, 2014, pp. 219–222.

[11] X. Xue, Z. Liu, T. Xue, W. Chen, and X. Chen, "Machine learning for the prediction of acute kidney injury in patients after cardiac surgery," *Frontiers in Surgery*, vol. 9, p. 946610, 2022.

[12] A. O. Akmandor, H. Yin, and N. K. Jha, "Simultaneously ensuring smartness, security, and energy efficiency in internet-of-things sensors," in *2018 IEEE Custom Integrated Circuits Conference (CICC)*. IEEE, 2018, pp. 1–8.

[13] J. Liu, Z. Zhu, Y. Zhou, N. Wang, G. Dai, Q. Liu, J. Xiao, Y. Xie, Z. Zhong, H. Liu, L. Chang, and J. Zhou, "A reconfigurable biomedical ai processor with adaptive learning for versatile intelligent health monitoring," in *2021 IEEE International Solid-State Circuits Conference (ISSCC)*, vol. 64. IEEE, 2021, pp. 62–64.

[14] S. Yin, M. Kim, D. Kadetotad, Y. Liu, C. Bae, S. J. Kim, Y. Cao, and J.-S. Seo, "A 1.06-μw smart ecg processor in 65-nm cmos for real-time biometric authentication and personal cardiac monitoring," *IEEE Journal of Solid-State Circuits*, vol. 54, no. 8, pp. 2316–2326, 2019.

[15] S.-Y. Hsu, Y. Ho, P.-Y. Chang, C. Su, and C.-Y. Lee, "A 48.6-to-105.2 μw machine learning assisted cardiac sensor soc for mobile healthcare applications," *IEEE Journal of Solid-State Circuits*, vol. 49, no. 4, pp. 801–811, 2014.

[16] K.-C. Chen, C.-Y. Chou, and A.-Y. Wu, "A tri-mode compressed analytics engine for low-power af detection with on-demand ekg reconstruction," *IEEE Journal of Solid-State Circuits*, vol. 56, no. 5, pp. 1608–1617, 2021.

[17] K. H. Lee and N. Verma, "A low-power processor with configurable embedded machine-learning accelerators for high-order and adaptive analysis of medical-sensor signals," *IEEE Journal of Solid-State Circuits*, vol. 48, no. 7, pp. 1625–1637, 2013.

[18] S.-A. Huang, K.-C. Chang, H.-H. Liou, and C.-H. Yang, "A 1.9-mw svm processor with on-chip active learning for epileptic seizure control," *IEEE Journal of Solid-State Circuits*, vol. 55, no. 2, pp. 452–464, 2020.

[19] H. Jia and N. Verma, "Exploiting approximate feature extraction via genetic programming for hardware acceleration in a heterogeneous microprocessor," *IEEE Journal of Solid-State Circuits*, vol. 53, no. 4, pp. 1016–1027, 2018.

[20] W.-M. Chen, H. Chiueh, T.-J. Chen, C.-L. Ho, C. Jeng, M.-D. Ker, C.-Y. Lin, Y.-C. Huang, C.-W. Chou, T.-Y. Fan, M.-S. Cheng, Y.-L. Hsin, S.-F. Liang, Y.-L. Wang, F.-Z. Shaw, Y.-H. Huang, C.-H. Yang, and C.-Y. Wu, "A fully integrated 8-channel closed-loop neural-prosthetic cmos soc for real-time epileptic seizure control," *IEEE Journal of Solid-State Circuits*, vol. 49, no. 1, pp. 232–247, 2014.

[21] Y. Wang, Q. Sun, H. Luo, X. Chen, X. Wang, and H. Zhang, "A closed-loop neuromodulation chipset with 2-level classification achieving 1.5vpp cm interference tolerance, 35db stimulation artifact rejection in 0.5ms and 97.8% sensitivity seizure detection," in *2020 IEEE International Solid-State Circuits Conference (ISSCC)*. IEEE, 2020, pp. 406–408.

[22] M. A. Bin Altaf, C. Zhang, and J. Yoo, "A 16-channel patient-specific seizure onset and termination detection soc with impedance-adaptive transcranial electrical stimulator," *IEEE Journal of Solid-State Circuits*, vol. 50, no. 11, pp. 2728–2740, 2015.

[23] J. Yoo, L. Yan, D. El-Damak, M. A. B. Altaf, A. H. Shoeb, and A. P. Chandrakasan, "An 8-channel scalable eeg acquisition soc with patient-specific seizure classification and recording processor," *IEEE Journal of Solid-State Circuits*, vol. 48, no. 1, pp. 214–228, 2013.

[24] M. A. B. Altaf, J. Tillak, Y. Kifle, and J. Yoo, "A 1.83j/classification nonlinear support-vector-machine-based patient-specific seizure classification soc," in *2013 IEEE International Solid-State Circuits Conference Digest of Technical Papers*. IEEE, 2013, pp. 100–101.

[25] X. Tang and W. Tang, "A 151nw second-order ternary delta modulator for ecg slope variation measurement with baseline wandering resilience," in *2020 IEEE Custom Integrated Circuits Conference (CICC)*. IEEE, 2020, pp. 1–4.

[26] M. A. Sohail, Z. Taufique, S. M. Abubakar, W. Saadeh, and M. A. Bin Altaf, "An ecg processor for the detection of eight cardiac arrhythmias with minimum false alarms," in *2019 IEEE Biomedical Circuits and Systems Conference (BioCAS)*. IEEE, 2019, pp. 1–4.

[27] A. Amirshahi and M. Hashemi, "Ecg classification algorithm based on stdp and r-stdp neural networks for real-time monitoring on ultra low-power personal wearable devices," *IEEE Transactions on Biomedical Circuits and Systems*, vol. 13, no. 6, pp. 1483–1493, 2019.

[28] A. Dabbaghian, T. Yousefi, S. Z. Fatmi, P. Shafia, and H. Kassiri, "A 9.2-g fully-flexible wireless ambulatory eeg monitoring and diagnostics headband with analog motion artifact detection and compensation," *IEEE Transactions on Biomedical Circuits and Systems*, vol. 13, no. 6, pp. 1141–1151, 2019.

[29] S. Sadasivuni, M. Saha, N. Bhatia, I. Banerjee, and A. Sanyal, "Fusion of fully integrated analog machine learning classifier with electronic medical records for real-time prediction of sepsis onset," *Scientific reports*, vol. 12, no. 1, pp. 1–11, 2022.

[30] V. Damodaran, J. Sanchez, T. Gupta, P. Bikkina, E. Mikkola, A.-M. Haidar, I. Banerjee, and A. Sanyal, "Ai-enabled fusion of electrocardiograph and demographics for prediction of acute kidney injury onset," in *2024 IEEE Biomedical Circuits and Systems Conference (BioCAS)*. IEEE, 2024.

[31] N. Tomašev, X. Glorot, J. W. Rae, M. Zielinski, H. Askham, A. Saraiva, A. Mottram, C. Meyer, S. Ravuri, I. Protsyuk *et al.*, "A clinically applicable approach to continuous prediction of future acute kidney injury," *Nature*, vol. 572, no. 7767, pp. 116–119, 2019.

[32] W. Liu, X. Liu, T. Jiang, M. Wang, Y. Huang, Y. Huang, F. Jin, Q. Zhao, Q. Wu, B. C. Liu, X. Ruan, and K. Ma, "Using a machine learning model to predict the development of acute kidney injury in patients with heart failure," *Frontiers in Cardiovascular Medicine*, vol. 9, p. 911987, Sep 2022.